

Tardigrade secretory proteins protect biological structures from desiccation

Supplementary Information

Table S1. SAHS proteins used in this study for expression in Figure S2.

Name	Uniprot ID	Host organism	Amino acid lengths (including secretion tag)
RvSAHS1	J7MFT5	<i>R. varieornatus</i>	169
RvSAHS2	J7MAN2	<i>R. varieornatus</i>	174
RvSAHS3	A0A1D1UKM2	<i>R. varieornatus</i>	146
RvSAHS4	A0A1D1UN89	<i>R. varieornatus</i>	171
HeSAHS4	P0CU42	<i>H. exemplaris</i>	174
RvSAHS6	A0A1D1UJP0	<i>R. varieornatus</i>	172
RvSAHS7	A0A1D1UQJ5	<i>R. varieornatus</i>	159
RvSAHS8	A0A1D1UJQ1	<i>R. varieornatus</i>	173
RvSAHS9	A0A1D1UKG0	<i>R. varieornatus</i>	113
RvSAHS10	A0A1D1UJR2	<i>R. varieornatus</i>	123
RvSAHS11	A0A1D1URS8	<i>R. varieornatus</i>	171

RvSAHS12	A0A1D1UNQ6	<i>R. varieornatus</i>	110
----------	------------	------------------------	-----

Table S2. Protein localization predicted by TargetP software, based on sequences from Uniprot files of Table S1.

Protein name	Other	Secretory	Mitochondrial
RvSAHS1	.0001	.9998	.0001
RvSAHS2	.0001	.9999	0
RvSAHS3	.0004	.9995	.0001
RvSAHS4	.0045	.9946	.0009
HeSAHS4	.0001	.9997	.0002
RvSAHS6	.0009	.9989	.0003
RvSAHS7	.9989	.0007	.0004
RvSAHS8	0	1	0
RvSAHS9	.9995	.0003	.0001
RvSAHS10	.9931	.0004	.0065
RvSAHS11	.0007	.9977	.0016
RvSAHS12	.9995	.0002	.0003

Table S3. Amino acid sequences of the SAHS proteins (after SUMO cleavage).

Protein name	Amino acid sequence	Mw(kDa)
RvSAHS1	APAEGHDDAKAEWTGKSWMGKWESTDRIENFDAFISALGLPLEQ YGGNHKTFHKIWKEGDHYHHQISVPDKNYKNDVNFKLNEEGTTQ HNNTTEIKYKYTEDGGNLKAEVHVPSRNKVIHDEYKVNGDELEKT YKVGDTVAKRWYKKSSSS	17.3
RvSAHS4	RPHDESKAQWTGKPWLKGWESIDGTPENWEAFVKAANI PPKDQA LYNGKQKTLLKYWKEAGEDHYHVQTSFPGTEHKMETSFKMGQEG TLSHDGVDLKYVCTEDGEQLITKINIPSKNQETIVTYTATGDDL EQTFTSNGVTGKRWYKKIHA	17.3
HeSAHS4	TGDAPKEWSGKPWLGKFVAEVTDKSENWEAFVDALGLPEQFGR PVKTIQKIYKQGDHYHHIFALPDKNFEKDIEFTLGQEVEIKQGE HIAKTKYSEDGEKLVADVSIPTKGKTIRSEYEVQGDQLIKTYKT GDIVAKKWFKKVANPTEAPAQAA	17.4
RvSAHS6	RPHDESKAQWTGKPWLKGWESIDKTPENWEAFVKAANIEPKYQS LYSGKQKAIITIYKEGDSHYHAQMTFPGTDHKKEWDFKIGQEGT YSMDGTEVKYVYTENGDLQDLSKLNIPSKNTEMTHTYKVTGDELE HIFTSNGATGKKWYKKVNNV	17.6

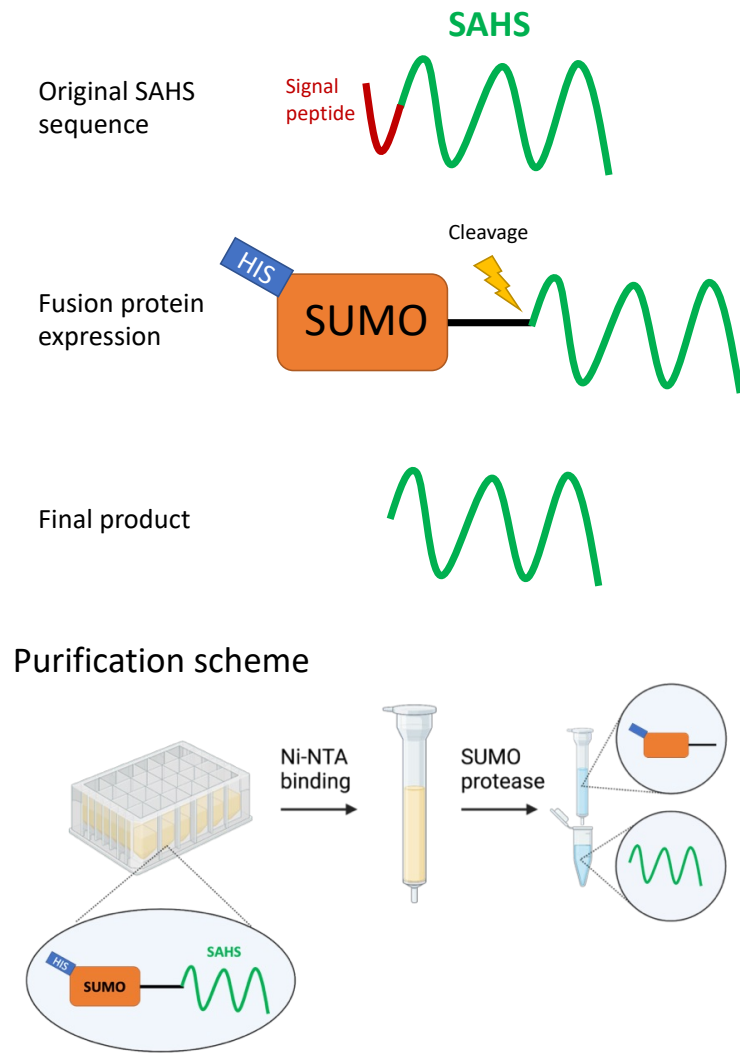


Figure S1. Sequence design purification, and cleavage of the SUMO-SAHS fusion proteins to yield mature SAHS proteins.

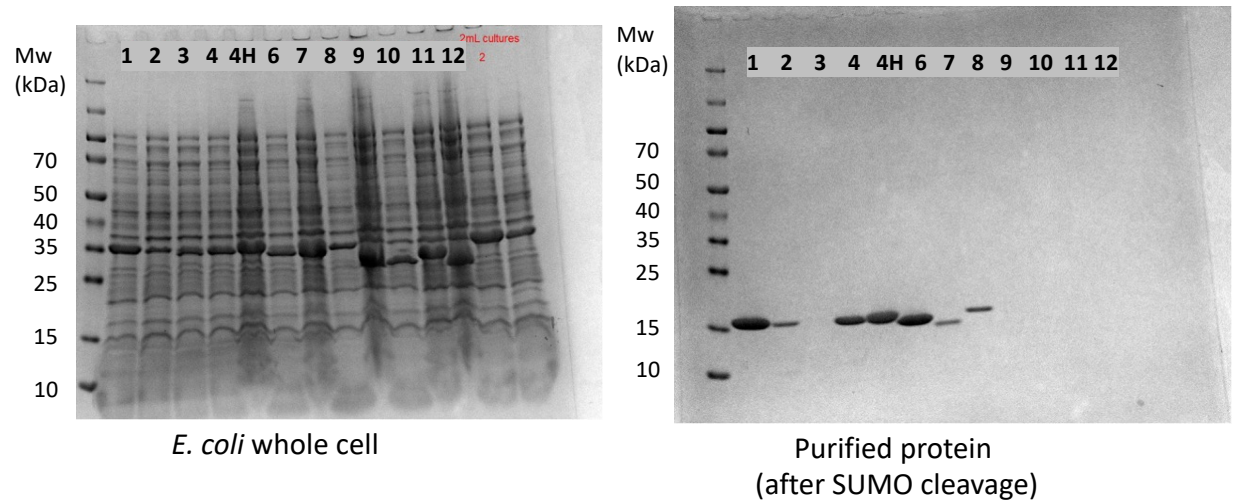


Figure S2. Expression and purification of the SAHS proteins from *E. Coli* host. Left: SDS-PAGE of *E. coli* whole cells expressing each SUMO-SAHS construct. Right: final protein products after cell lysis, purification and SUMO cleavage. Each number indicates corresponding RvSAHS protein, and “4H” indicates HeSAHS4. RvSAHS1, 4, 6 and HeSAHS4 were highly expressed and efficiently purified.

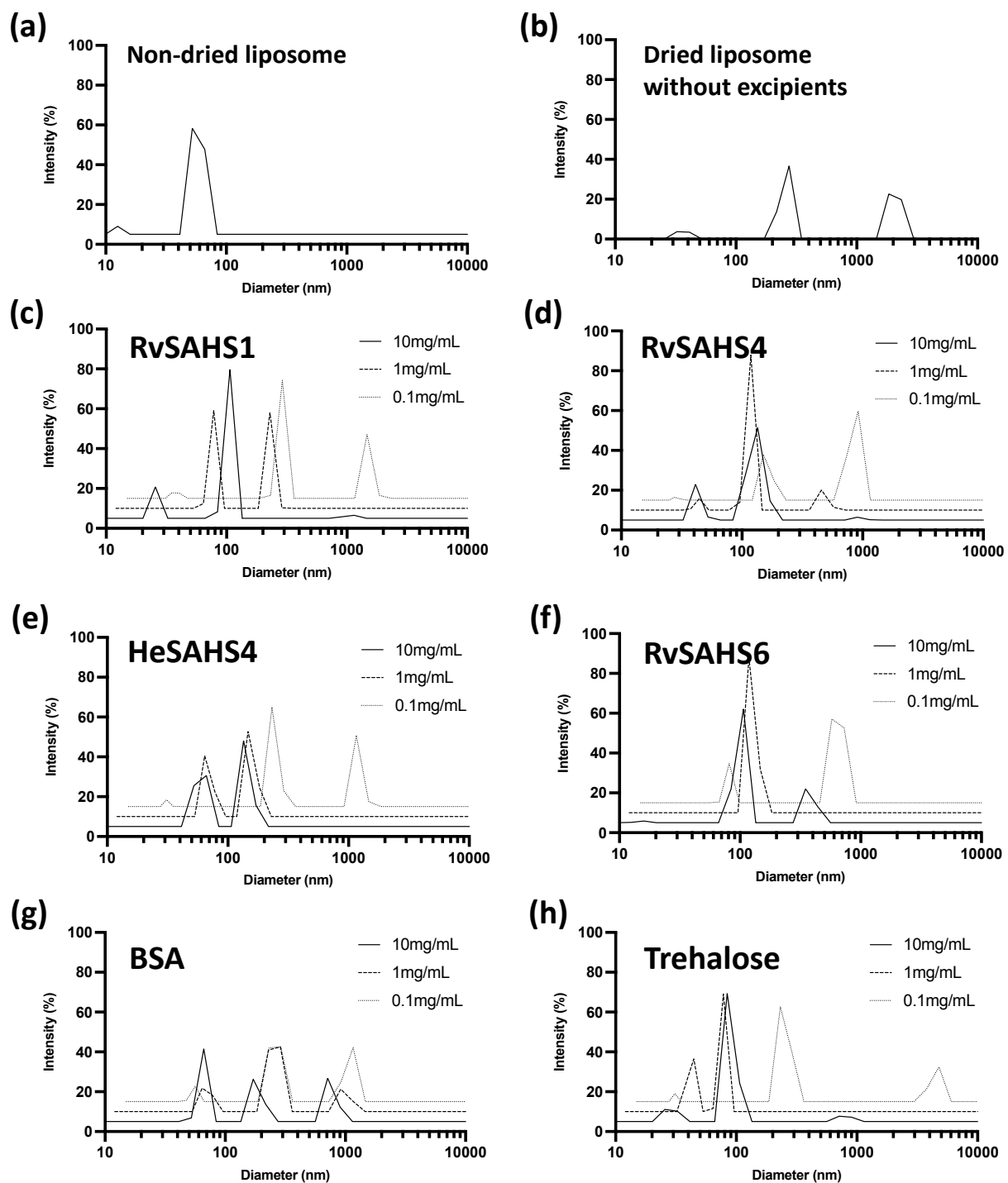


Figure S3. Data from a repeat experiment of that in Figure 2 showing that SAHS proteins stabilize liposomes from desiccation-induced damage. 1-palmitoyl-2-oleoyl-glycero-3-phosphocholine (POPC)-based liposomes at 1.4 mg/mL were dried with and without the addition

of SAHS proteins or BSA at varying concentrations of 0.1 to 10 mg/mL, and their size distributions were measured by dynamic light scattering. (a) Size distribution of non-dried POPC liposomes (b) Size distribution of POPC liposomes dried and rehydrated without additives. (c-h) Size distributions of the liposomes dried with (c) RvSAHS1, (d) RvSAHS4, (e) HySAHS4, (f) RvSAHS6, (g) BSA and (h) trehalose.

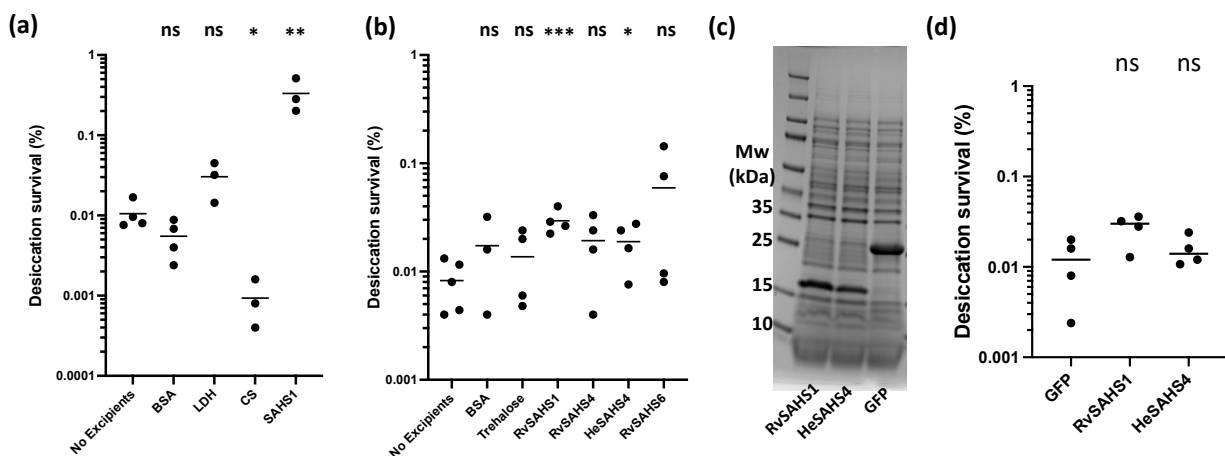


Figure S4. Protection of bacterial cells against desiccation by SAHS proteins. (a) Survival of *E. coli* cells dried for 48 hours with 0.5 mg/mL of BSA, lactate dehydrogenase (LDH) and citrate synthase (CS) as control proteins, and SAHS1. (b) Survival of *E. coli* cells dried with 0.1 mg/mL of extracellularly added SAHS proteins and control excipients. (c) SDS-PAGE of the whole *E. coli* cells intracellularly overexpressing heterologous RvSAHS1, HySAHS4 and GFP. (d) Survival of dried cells intracellularly expressing each protein. Individual data points represent independent replicates and lines represent the mean survival. The student's t-test was used to determine the statistical significance between the negative control (no excipient) and each group, which is indicated as asterisks. * $p < 0.05$; ** $p < 0.01$; *** $p < 0.001$.

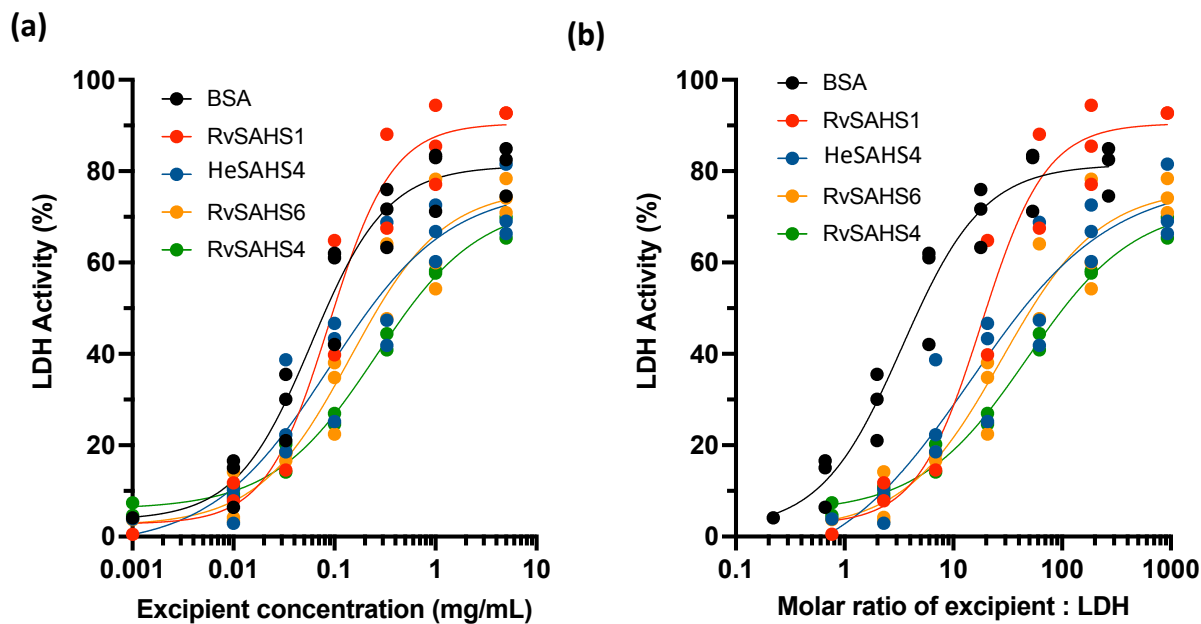
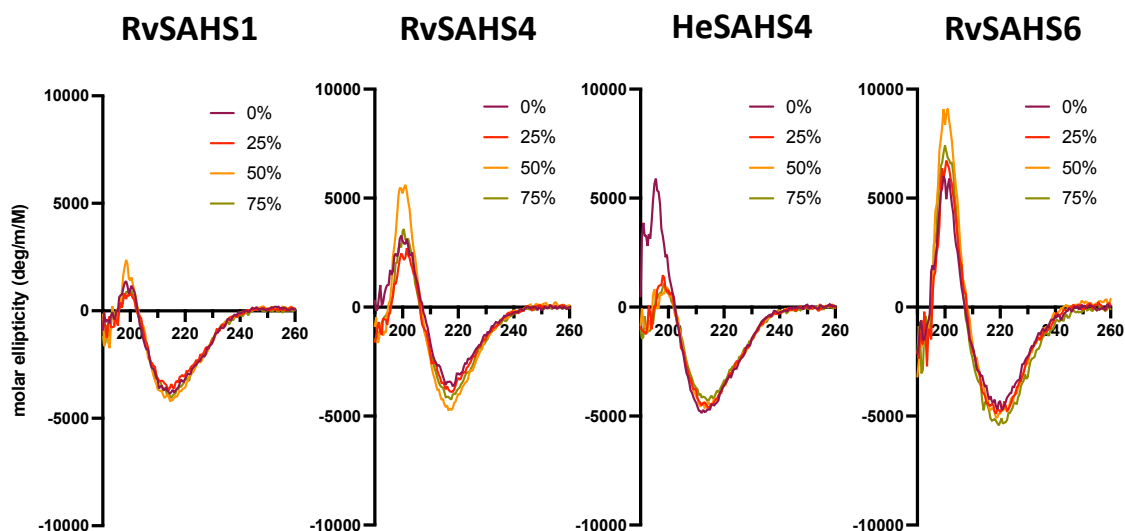


Figure S5. (a) Tardigrade SAHS proteins and BSA protect lactate dehydrogenase (LDH) enzyme activity against drying. LDH (0.01 mg/mL) was desiccated and rehydrated in the presence or absence of SAHS proteins and BSA. Percent activity was determined using non-desiccated control samples stored at 4°C as the reference to compare activity. (b) The data from the same experiment as (a), using molar ratio between protein excipient and LDH as the x-axis.

(a)



(b)

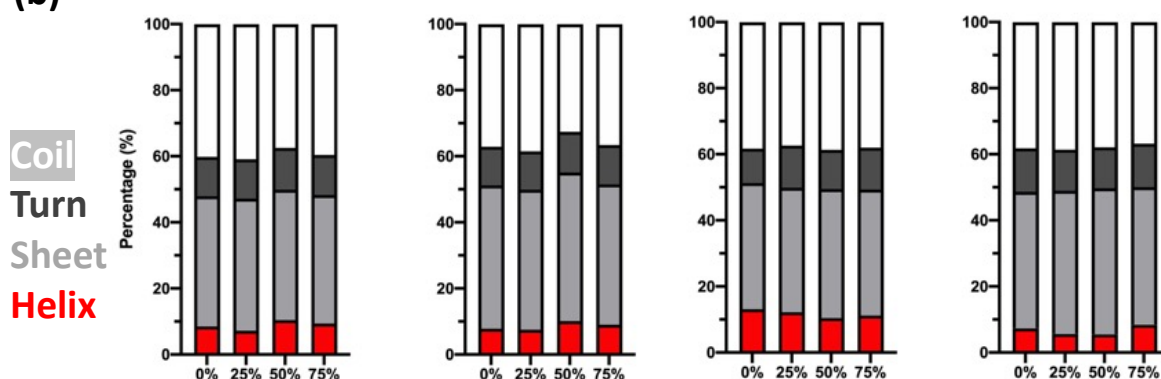


Figure S6. Effect of glycerol on SAHS protein structure. SAHS protein secondary structures upon glycerol addition were determined using circular dichroism. (a) CD spectra of SAHS proteins upon addition of increasing amounts of glycerol from 0 – 75%. (b) Secondary structure compositions of SAHS proteins under different glycerol level, calculated from the CD spectra.

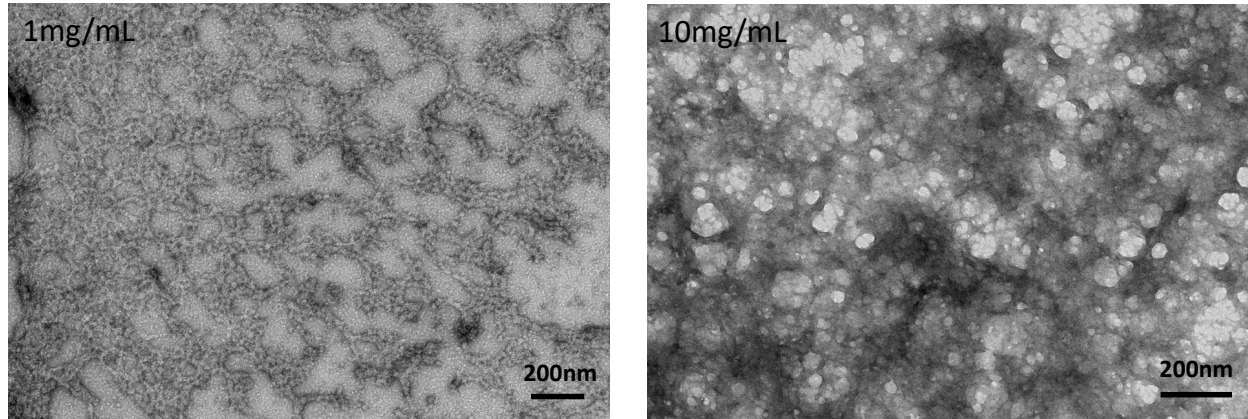


Figure S7. Transmission electron microscopy images of the fibrous network structure formed by RvSAHS1 proteins dried at 1 mg/mL (left) and 10 mg/mL (right) concentrations. Scale bar = 200 nm. Previously, TDPs belonging to the CAHS family have been shown to form filamentous structures upon dehydration both *in vitro* and *in vivo*, and these proteins may adopt increasingly helical structures with loss of water [1, 2]. It is possible that although structurally distinct, SAHS and CAHS proteins share an ability to form higher order structures under dry conditions.

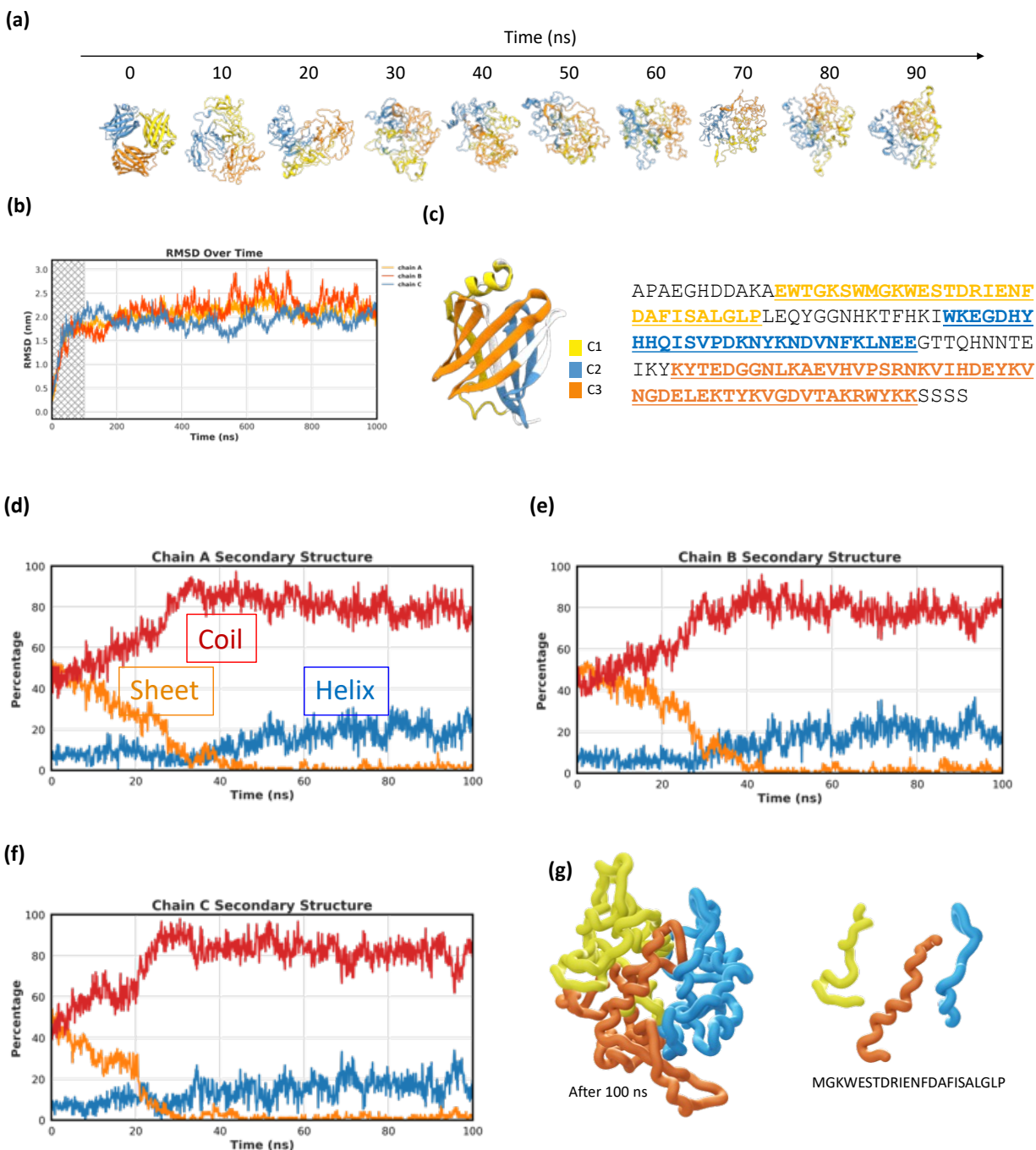


Figure S8. MD simulation of an RvSAHS1 protein trimer. AlphaFold was used to predicted the structure of three SAHS1 proteins, giving the T=0 structure in (a). This structure was used as a starting point for a molecular dynamics simulation for 1 microsecond. (a) Changes in the structure of the RvSAHS1 trimer during the first 100 ns of simulation. (b) Root mean squared

deviation (RMSD) relative to the starting structure over time during the entire 1 microsecond of MD simulation. Different colors indicate each monomer chain in the trimer. (c) Mapping of conserved segments C1-C3 of the RvSAHS1 sequence as defined by Yamaguchi et al. [3] prior to the solving of the SAHS1 structure. Amino acid sequence of RvSAHS1 is indicated, with C1 motif represented in yellow, C2 in blue, and C3 in orange, respectively. (d-f) The distribution of sheet, helix and coil conformations of amino acid backbones for each of the three SAHS1 proteins in the simulation. The sheet/helix/coil classification is based on the psi/phi dihedral angles of each amino acid, and not on hydrogen-bonding patterns that may or may not be present. (g) State of the simulation at 100 nsec (left), and a segment from each of the three SAHS1 proteins represented to illustrate the formation of short helical segments. During the course of the high-temperature simulation, helical segments throughout the proteins are unstable and present transiently.

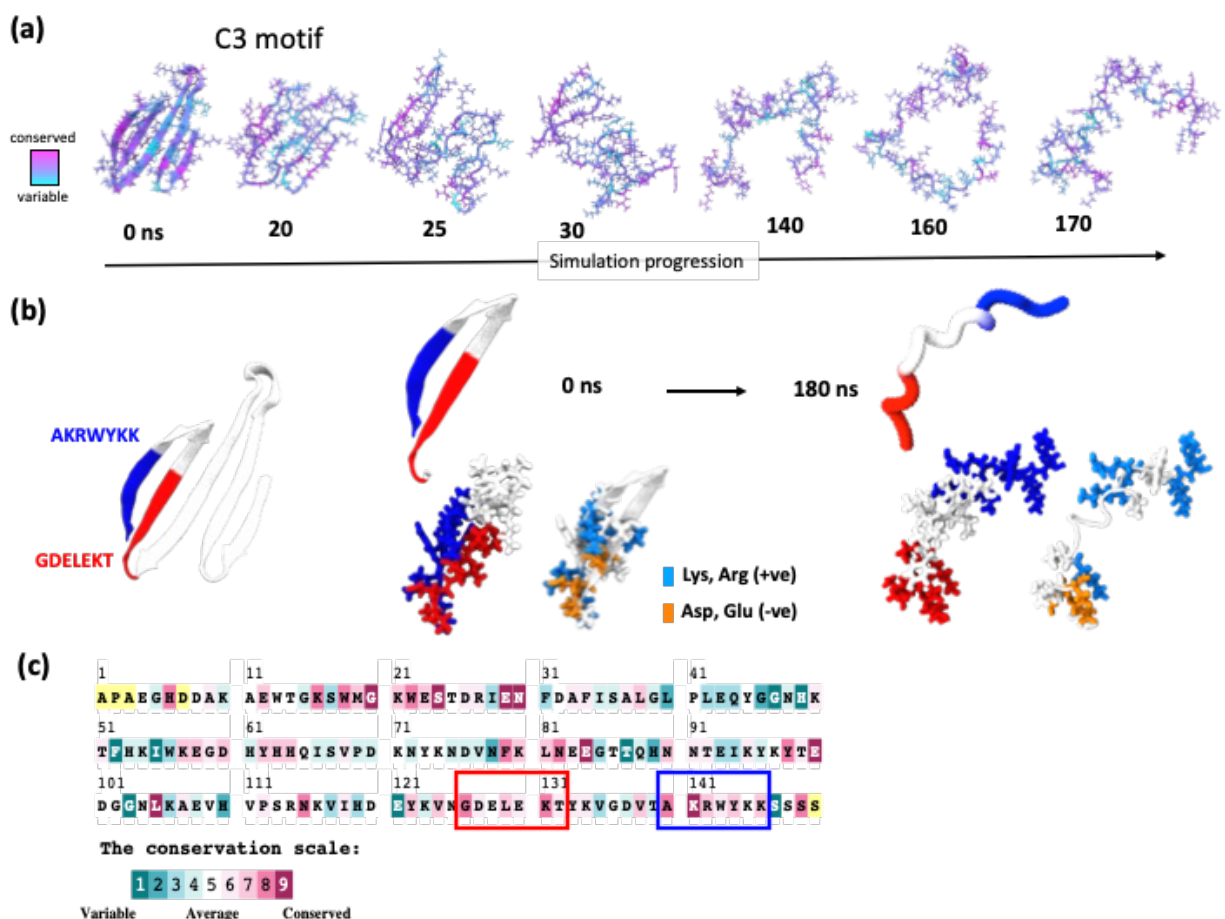


Figure S9. MD simulation showing structural changes in the conserved C3 motif of RvSAHS1.

(a) Representative structural changes in C3 motif during the first 170 ns of simulation. Color scheme indicates the degree of evolutionary conservation, which shows that this motif is highly conserved among the SAHS family. (b) Close-up representation of the C3 motif sheet-to-helix structural change. Highlighted in blue and red are two highly conserved regions found within the beta sheet region that directly interact through ionic bonds. Structures of these regions at 0 and 180 ns are indicated, along with an additional depiction of the same regions in which positive residues (Lys, Arg) are highlighted in cyan and negative residues (Asp, Glu) are highlighted in orange. (c) Evolutionary conservation analysis of the RvSAHS1 sequence. Red and blue boxes indicate the same sequences depicted in (b).

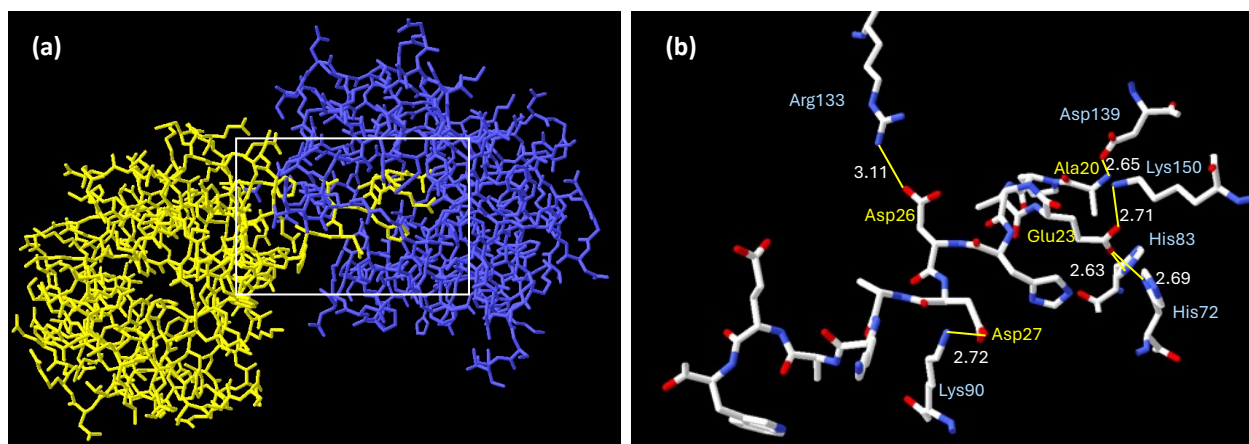


Figure S10. AlphaFold-predicted insertion of the SAHS1 N-terminal tail into the SAHS1 cavity. The AlphaFold-predicted structure of three SAHS1 proteins indicated that the N-terminal ~9 amino acids of mature SAHS1, which are predicted to be unstructured in a monomer [4], might be able to occupy the cavity of a second SAHS1 protein. The T=0 nanosecond structure in Figure S8(a) shows the trimeric structure predicted by AlphaFold, which contains three different insertions of an N-terminus into the cavity of an adjacent SAHS1 protein. These differ in detail, and we regard the complex in this figure as the most structurally plausible. (a) A SAHS1 protein (yellow) with an N-terminal tail located in the cavity of a second SAHS1 protein (blue); this is a close-up view of two of the three proteins depicted in Figure S8(a), T=0. (B) An expanded view of the region in the box of panel (a) in which the first 14 amino acids of the yellow subunit are shown (Ala20-Trp32, with interacting amino acids lettered in yellow) and select interacting amino acids from the blue SAHS1 protein shown and lettered in light blue. Also shown are the distances, in Angstroms, between oxygens in one side chain and protonated nitrogens in another, in cases of possible hydrogen bonding. Amino acid numbering is relative to the first amino acid in the translated sequence (as in Figure 1), such that after removal of the 19-amino acid signal sequence, Ala20 is the first amino acid in the mature SAHS1.

We note that when Fukuda et al. solved the structure of SAHS1 [4], they removed the N-terminal 10 amino acids of the protein because this segment might interfere with crystallization, and the cavity was filled with solvent molecules. The crystallized form of SAHS4 included an extra serine at its N-terminus, which may have disrupted insertion of the N-terminus into the SAHS4 cavity, given the tight packing and specific contacts made by the N-terminal amino group in the SAHS1 model of panel b [5]. The human liver and heart muscle fatty acid binding proteins, which are otherwise similar to the SAHS proteins and possess a large cavity, lack these N-terminal tails (see Figure 1b).

Supplementary Discussion: sequence annotation of SAHS9, 10 and 12.

The “short” SAHS proteins, SAHS9, 10 and 12 from *R. varieornatus* are truncated at their N-termini relative to other SAHS proteins. The Uniprot versions of SAHS9, 10 and 12 lack signal sequences, could not be expressed in a soluble form, lack residues that appear to be important in forming the hydrophobic core in SAHS1 and SAHS4, and for SAHS9 and SAHS12 began with a methionine corresponding to a methionine also found in SAHS3, 7 and 8. We therefore explored whether these might be incorrectly annotated and examined the genome sequence of *R. varieornatus* for upstream coding sequences that might have been overlooked. The results of this analysis are that the SAHS9, 10 and 12 genes encode proteins that may extend in the N-terminal direction further than the annotation would indicate, and that the new predicted protein sequences align well with N-termini of other SAHS proteins. However, we have not found clear-cut start codons for *SAHS9* and *10*, and SAHS12 may be much larger than the other SAHS proteins. The annotation below is intended to be a work in progress.

The *SAHS9*, *10* and *12* genomic regions were obtained from Genbank accession # *BDGG01000001* (contig 1), a large contig from the *R. varieornatus* genome [6]. Relevant genome sequence fragments were obtained as reverse complements, then copy-pasted into Microsoft Word, and visually scanned for the presence of splice acceptors upstream of putative start codons for ORFs that translate into the Uniprot sequences. Because all of the SAHS genes in *BDGG01000001* are on the anti-sense strand, we generated the reverse complement of this ~ 9Mb sequence for presentation purposes. The numbering used below is according to this reverse complement. Upstream regions of *SAHS9*, *10* and *12* were also copy-pasted into the ExPASy Translate Tool (<https://web.expasy.org/translate/>), translated, and checked for long ORFs. A visual scan of the translated sequences revealed a pattern of tryptophans and other amino acids

that align well with the N-terminus of other mature *SAHS* genes (Figure 1B), but which are not found in the annotated sequences of these genes.

We also examined the intron/exon boundaries of these SAHS proteins and compared them to regions encoding other SAHS proteins to further validate the proposed mature amino acid sequences.

***SAHS9* analysis**

The *SAHS9* protein sequence is most similar to *SAHS10*, 2 and 8. *SAHS9* is also adjacent to *SAHS2* and *SAHS8* in the genome and is in a ~30 kilobase region that codes for *SAHS11* plus *SAHS10* (also adjacent) and *SAHS7* plus *SAHS1* (also adjacent).

When the *SAHS9* genomic sequence is aligned with, for example that of *SAHS2*, there is a putative splice acceptor in *SAHS9* DNA upstream of the annotated start codon at the same position as a splice acceptor annotated in *SAHS2*. Moving upstream, there is a putative splice donor in *SAHS9* such that an intron of 79 bp is predicted, similar in size to the 82 bp intron in *SAHS2*. Moving further upstream, there is a predicted exon encoding a protein segment that aligns well with other full-length SAHS proteins, including Trp residues that help define the hydrophobic core. However, the predicted splice acceptor upstream of this exon has the sequence . . . TCCTTCTTACCG, lacking the canonical AG, and yet further upstream it is difficult to identify a splice donor and start codon that would align with other *SAHS* genomic sequences. It is possible that *SAHS9* is a pseudogene, that this region of the sequence contains one or more errors, or that some other mechanism operates to express this gene.

Below is the genomic region encoding *SAHS9*, 2 and 8.

```
2575501 atttttcgcc tgtacagaca taagctgtta gagctgatgg agacacacct agatctcggg
2575561 ttgacaccca atgacacggt aatgatcctt agaccattgt ccgaaaaatt gctcatcacc
2575621 gttccctgta tggaaaaaaa ctggccttggc gggtaaccttc gtgaacaata gtatgtcagt
```

2575681 tgagtttttcg gtgagtcata aggggcagat agccgcgtgg cggaagcagc tgttttcggcc
 2575741 tgtactgcaa accatgcata ggaaatttgg t~~taaaaaa~~acg actttttccag tttttttccc **TATA box**
 2575801 tacatggata tttccgccca aatttagcca tccattcggt tgtagaatgt ttcagcatt
 2575861 cgatacctta aggcagctc ttgataacta cataagcggg ttcaagagtt cgactaacgc
 2575921 cctccagaa aacgtcgttt cctgaacagt ttagaaaata cctcggaaac gcccaattaga splice donor
 2575981 aaaaaacagg cgtcagttat gctgtacatt gctgcaacgg tgtacaggtc gaccgagcca
 2576041 acggaatccg aataacatcc gaataatatc cttcttaccg gcgctgccat cgccattctc end of signal
 2576101 atcgaagacc ctgctgacga aaaaggagca gaa~~ttgg~~accg gaaaaccgtg gctggggcga exon 2 **Trp codons**
 2576161 ~~ttgg~~gtctctg tacccgagca ggacaaaaac ctggcacagt tcaagaggaa gcttcgtaag
 2576221 ttttacgtct cctgtgtgac tttgatcttt ctgtacgatt gatgacgttc ttcccgata
 2576281 tatatcgttc acagagctgc ctatgagcca tccggaagtc aatctcaact ctactgtctt **SAHS9 "start"**
 2576341 ggtcaaccac ctcaagaagg gagatgaata ccatcacaag attatcatca aagaatatta exon 3
 2576401 caccaatcac gtaagtttat aaccgttagc gcgctcttaa aaaaagcaaa atggtcacgc
 2576461 gaaaacgttt tttaggtcgt ttacaagctg ggcgagcagt cacccggtc gtacgacggt
 2576521 ttgtcctata gtgtaaagta tggagagaaa gatggcgctg tgggtggaac ggccattacg exon 4
 2576581 acaggcacca aagaccagcg tctcaacata accatgcaca acgtctacaa gctcgaagg
 2576641 gatcgtcttc tcaagagctc caccatcgac ggagtaaacac tgaattgcca tcacaagagg
 2576701 cgcattc~~tgaa~~ gctgtgacg tctgttcagt tcttcgactt ttatcgatat tcttatagtc
 2576761 ttgatcaacg cttgagtaaa ggtgtttcaa gatgcataaa gactttcttc gtccttggcg
 2576821 aatccttata ctcatctct cgaatcaaga tatccattcc atcggcagaa ggagagattc
 2576881 tccgctttcc acacttgcgt gggtagactc gtgtagagcc gcgctatcg cgtgaacat
 2576941 cgagaaagggt tcgaagcttg gcttagagtt ctacagcggg caccgggacaa gatcagatac
 2577001 ggcgcaagggt tgttttcccc agcatgcaga ccgttatgac acatagttga ctttgatgcg
 2577061 actggtgtga ttgggaagaa tgtaacgctc caatttcgc ctaagggtga atcctaaggt
 2577121 atacgtacag tagacgcaaa cagtacagac tccctcagca acggtacttc ctggccgta **TATA box**
 2577181 ~~ataaaa~~atcaa ggttcgggtt ccttccaacc tgtacctctt tacttctgtt aactttctca
 2577241 cggagaatac tcgcagaacc atgcatcgat ttgtccttgc tctcgtcgtt tttgcccgtta exon 1
 2577301 aacttgaaag cttcttaaga gatttaccgt ttgtgtgct atgaaagag acgagcatga Intron 1
 2577361 gctaaaagg catcgttaaga aacgtgcgtg gctatatatg tacattttct cctggccttg
 2577421 caggtgctgc catcgtctgg gccgctgatg acgctgctca cgaagaaggc gtagaatgga signal sequence
 2577481 ctgggaaacc gtggatgggc aaa~~ttgg~~aat cccagccatc gaaggacgag aacgttgagg exon 2
 2577541 aattcaaaa gaagctccgt aagttacttt gcatttgcac cctctogtta gttagtttt **Trp codons**
 2577601 ttagtgttca gtgcagctg gttgtctggt ggattcgtcg aattccccgg cctgatattt
 2577661 tttgcatagc tttatagatt taccggttca gatccgtaca agcgagaaac caagacacct
 2577721 atgtttgttt gcagagcttc cgatgagcca ctcggaatg aacaaaaact ccaaagtttg
 2577781 gatccatcac tacaagaagg gagacagata ccatcacaac atcatcatca acgacgccta exon 3
 2577841 ttacaaaaac gatgtaagtc cgcgaacttt cccggttaca ttgtttctta cgtcttttgc
 2577901 gcacagatca aagaaaatta ttttcggctt tgtagatcgt cttcaagctg ggtcaagagt
 2577961 ccgcccgttc gtataacggc tcatctttca gcgtgaagta cgaggacaaa gacggcgctc exon 4
 2578021 tagtcggaag cgtccactac actggcacca aagaacagtc tcttgacaag accatcaaca
 2578081 acgtcttcaa gctcgaagggt gaccatctgg ttaagacttc caccatcgag ggagtgaaca
 2578141 tgaagcgcca ctacaacaa cgccagt~~tgaa~~ gttgtcgttg cggctaaatt tttcctttc
 2578201 tgcaaatcca tgcccgttt gtgcagcttc tctcgtctcc catcgttcta aagatttttg
 2578261 cagactagag ttatcagggc ttgtttctgt ttctcgtttc atcctcgtat tttcttttgc
 2578321 ttcaccggat acagtaaaagc tgcggtttcaa agccagggtt tttatctgcc tgttggtcgg
 2578381 acggattgtc ggaccaactc agatatcgat cgggctgatt gtaaacagat actacgtatt
 2578441 ttctcgtact ctgcgactg gctaacgtta ggttatcagc tctaaccggt gatcagagaa
 2578501 gttttaaaag caggcacgac atactttaaa ttctcaaac aacagtactt tccccatcag
 2578561 atgaagcata aagcgggttt tcccagcaaa gacgcttcag cccatggcca attgacctt
 2578621 ggccgaaggc tgctggctac gaaagcgtg agtaatgata agtactcgta ctctattgtt
 2578681 caactaagaa acctccgaat gtaaccctaa ggagaacgac ttcgtgccaa cttgatctta
 2578741 gactgcagaa taaaccag~~ta~~ taaaa~~t~~caaa ccttcgccat ttcacagtac aaagcacgtt **TATA box**
 2578801 ttaaaccttt ccagccactt tcttcacgta gaagtcgagc cgcaagcatg **SAHS8 ex.1**
 2578861 tagctctcgc tctgtttgcc ggtacgtcga cagacaatta aaattttggt gctttttagt
 2578921 atcatagggt aatgcaagac gttgactcga cttgtgtgga tgatcacatg agcatgtgat
 2578981 tcatagtgtga tttcattggt ctgttgcagg ttgtgccgtc ggttgggctg gcgatgatgc
 2579041 cgctcoatgaa gaaggagtgc act~~ttgg~~acctc caagcct~~ttgg~~ tgggcaagt **Trp codons**
 2579101 cccggagaag gatgaaaacc tcgtggagtt tctcaagaag ctca~~gtac~~gg tgtatagctt
 2579161 tctcttctt cagtattttc tgttctggac acatatacata aacagggtcc tcgctccagt
 2579221 ccccgctcc cttagtctta gaaaatttag agttttcag ctttacttct gttcacagat
 2579281 gttcccttag accactctaa aatgaacgac accgtcaagg tccacctcaa ccaactaag exon 3
 2579341 aaaggagacg attaccacca caagatcatc gtcaaggagg ctgagtacaa gaacgatgta
 2579401 agtttgaccg ctttcgatga gttgaccctg cagctagatg acccctttcg gaagtctatc
 2579461 ctatgggggt tccgactgac actagacacg taatatctgt ttccgattttt aggttgtctt
 2579521 caagtttaggc caagagtccg ctggttcgta caacggttcg tcttcaccc ggtacgaagg aacagagcct exon 4
 2579581 agataaggat ggcgcactgg tcggaacat tcaactacac ggtacgaagg aacagagcct
 2579641 cgacaagacc atcaacaacg agtacaaggt tgaaggcaat caactgggtc agacctcaac
 2579701 cctcgaagga gtgacacaca agagatacta caacaacgc aact~~tg~~agggt gttcttgcg
 2579761 ctatatgtgt cttagtctcg ccaagttttt cctattttcg catctttttg ctttttctca
 2579821 tcattcttcc agtctttatg ttgcgctgtt ctcactgtac tttgctcaag cccatttcca
 2579881 gcaacaagtg ctttattcac gtcccagaac cagctttccg ctcgctggtt acctattcgc

```

2579941 ggaagaaatc atccaacatg accaatactg cttctgagcc gataaagtca acgatttctg
2580001 tgctggattc gatttttcga tgtagatact ggacttgact ttgacttgta cggagcgaca
2580061 ccgagcgcag caggaacgca agaagaaaac caagcagata ctttaaccg cttcaaattt
2580121 agagtgggtc ttccacgct gccactgcat tgaccggtgt tttgtttcct gaggtagact
2580181 gatccctctc ctcgaggttt caataggttc gagaacggga aagcgttgta gattacggga

```

SAHS10 analysis

SAHS11 and *10*, shown below, are adjacent in the *R. varieornatus* genome and about 5 kilobases from the *SAHS2*, *8* cluster. The *SAHS10* annotated start codon lies within a putative intron corresponding to the second intron in *SAHS11* and other *SAHS* genes. *SAHS10* encodes two of the three conserved tryptophans near the N-terminus, while the first tryptophan is replaced with a structurally plausible arginine. Upstream of this coding region, at the position of the splice acceptor found in most *SAHS* genes, a potential splice site is mutated, reminiscent of this site in *SAHS9*.

```

2568721 tcgtctgccg cgtgcacgat gccaggaacg aaaaagcaag ctaggttcag agccaacctg
2568781 ttcatcacaca agtgctatcc agctatcctg ctctgcagac ttttaggcta tcttcgcacag
2568841 tctccatttc tgtaactgca agttagaacg cctcaattgt catgcggcga tttcttcgca SAHS11
2568901 atcttctcat atttgccagt atgaaccttc ccacacctgt aacgttatgt gtttatgatt
2568961 tttctatttt cgtcctttga atcagaagcc tgactttcca aggataatat aagtaaacga
2569021 aatgtaatta ggtggaccga agggatctag tgttttcccc gtccgattgg cgaatggctg
2569081 ctgttttggg taattatgat ttccgacgaa tcgataagag cttggctcaa gggactgtat
2569141 tcacccacag cttgatcctt tacaggtgcg gcagtctgcc tggcagagca cgtccctggc exon 2
2569201 catgaggaag gagccgaatg gactggaaaa ccatggctgg gcaaatgggt ttccgttccc Trp codons
2569261 gagaaggacg taaacgtact aaacttcata acagagatcg gtccagtgcc tgaatgcata
2569321 acttcagccc tcgtggtacg ctcagcggat ggcacgggac attcgaaatg gaatgaattt
2569381 tcacaggtgt cgctgcgagt catccggaac ttctcccat cgttacggtc ctcgtcaacc exon 3
2569441 attacaaaaa gggcgacgag taccaccaga gactgcgctg caaggaagta gctgatcttg
2569501 atgatcacga cgtaaagtac atacacggta ctcccttgac ccaggcttaa ggaaggcttc
2569561 ggaccgacgt taacgttaag gaacctgtac tgtagattgt ctacaaactg ggccaagaaa exon 4
2569621 ccaagaacgt ttttaacggt accaccttca gtgttaagta cgatgagaaa gatgacgctc
2569681 tcgtcggaca agtcatgcta ccctcgaaca acgcgactta caagaacgag ttcaaggctc
2569741 aaggggactt ccttgtcaag gtatcgcagc ccactttgaa ttccgctca gccattatgt
2569801 cactggtcac atcttttttc gcttgttgca gacctctgac gtcatggaa ttgtccaaa exon 5
2569861 acgatattac aagagacgga actaaatttc aagctggtgc cgaggttcag tctcagattt
2569921 tgtcttttga atcaagctcg cttgcgtggt tgagttgtcc ccagagtaaa gtcacatgtc
2569981 gttcagttgg cgtgtcgata gaggttcttg tgcttagtct ttagtgctac aagattttcc
2570041 cgagcagacg ggtggttcag tcggtttcca cttttttccc acattatccc gcatactctc
2570101 gtaacacaga caaccactgc cagaaaacgc gccggggcgc ttgaccagat cagatgggtg
2570161 gcaaagcagg caatcataat tcatacagcca acctttgaaa ccacgttttt tcccccgag
2570221 tgtcctaata gcgaatgac aatgcttgag gtcgaaaaaa agtgactaca ggctactcac
2570281 aataagggca ggtcaacact atatatgcag gcctctcctc aaaccttcca ttagtttctc
2570341 taccacatcg actttcttac atagccagct tgaacgatgc atcgatttat ccttcttctc
2570401 gcagtctttt ccggcaagat cgagctcata tcgggatatg gttccttata ctcgggagat
2570461 ggctctgtca tcggttggtc ccagccgcta actttccgtg tgcgacgtca ctgcgagaag
2570521 catcggcagg cagaatccgc actgacgcca taagaaagct taagcaagag gagttcgggt
2570581 gtcaagatgc tggatgggaa gctgtctgcg tgttttggtc gttgtgcatg tactcgtact
2570641 gtcgatgatg tgtttcgcgg gtgtggcctt tatctgggcc gccgaagacg ctgttcacga
2570701 agaaggcgtg gaacggactg gcaaacctg gatgggcaaa tgggtcgcgc ttctgagaa Trp codons
2570761 ggacgaaaat cacgagggac tcaagaaaaa gctccgtgag tacattcgtg ttggcttctg SAHS10

```

```

2570821 accttcattc gtcagttttc ctgcacaatc gtcgatgtga tgtatgagcc accatgggga "start"
2570881 tgcgatctgc agatatcccc ttgagtcacc cgcattctgaa acacaacaac agagtgtggg
2570941 ttaacaccta caagaaggga gacgaatacc accacaagat tattatcaag gaagccggct
2571001 ataccaatga tgtacgtatg cgaagccatt atgattatgc aaactgccga acgctgcatg
2571061 gctttaatct ttccacacag tacgtgcgta ctgagatctc ttgcatacct gagactgatt
2571121 ttcaggttgt cttcaagctg ggtcaagagt ccgccggctc gcataacggc tcatotttca
2571181 gcttgaagta cgaagacaag gatggcgccct tggtcggcac cgtccatcgc accggcacca
2571241 aggaacagcc cctggacaag acgatcaaca acgtcttcaa gctcgagggt gaccatttag
2571301 ttatgacctc caccatcgac ggagtaacca tgaaacgcta ctacaagaca cgaacgtgaa

```

SAHS12 analysis

In the annotation of Scaffold 1 of the *R. varieornatus* genome, the ORF upstream of *SAHS12* (*RvY_02619-1*) encodes a protein whose C-terminal region aligns well with the N-terminus of the mature SAHS proteins. A splice donor is present near the end of this sequence that corresponds to intron 2 of *SAHS2* and other well-annotated *SAHS* genes.

This region thus may encode a large protein with the sequence

MTQPMSFAQCSADRGKHS^{GTTI}WTLLRIYLACQKAILRSKLRLRAPLFPTVEPNPAPIQN
 AAPAPSAAQRRRNFAASHAANVDLPGSVWHGETWGDQHDPPNRLAADVDNFDWRSK
 FWLGKWSSIPEKDQNLEAYLAVM^{gvd}MNHPNMKKDQ^PVTLQTFKKGD^{KY}HHKIVVEE
 AGYINDVIFRLGRETPGSYNGQQITVNYEEQGGALVGTVKYPAHNKVIHNTYEMDGQN
 LAKTSECEGVVHKRWYNKQ^{QN}, where the black amino acids are from *RvY_02619-1*, the
 “gvd” is glycine-valine-aspartate arising from the splice junction and segment upstream of the
 annotated SAHS12 start codon, and the brown amino acids are from SAHS12 as annotated in the
 Scaffold 1 annotation.

```

2002141 gatgagcaac aagtaatggc tcggtaccag ctaagacctg aggcaaaatc aacgcggatg
2002201 gatgcagatc tatttcagtg aacaaaggac ggaagatttc tgatgggagg aaaagtagta
2002261 cagtgtataa ataattccgag aaagaaaatc aaattctgac ttccagagtc atctgagatg start of
2002321 actcaaccga tgagtttcgc acagtgcctg gcggaccgcg gtaaacattc cgttaccacg RvY_02619
2002381 atctggacgc tgctgcgaat atacttgccc tgccaaaaag ccattccttcg atcaaaatta
2002441 aggcctacgag gtaaacgtca caattcggac gggccaattt tctcgtcaca attcgggcgg
2002501 ctcgaaaagt tgatacgtta tttgctacgc tgtattgatt gatcaccgta gatcggttga
2002561 tacaacttta ggctttttta catttcgcat acccctcttc ctcccaccgc tgactccgca
2002621 actctttgac atcttttcgat atctcaacct atcacaagag atagaagaga ggatgttcta
2002681 ccctgggaag caaaaactag gcagtttgga gcagaaacag ctgagataca gaccgcccaa
2002741 attgtgacga gaaaattggc ccgcccgaat tgggacgttt acctcgtaac gattatgtgt
2002801 tttgtcttct aatcagctaa tcaagtcatt ggttttcatg aggattatgt tgatgcatga
2002861 ttctctgagc ttttgacagg ccgtaccgtg cttcacggag tgtttacccg ccgaatactg
2002921 ccaatgagtc attagaagca ccaggattgg tctgttactc tgtctattc aaatcaggcg
2002981 aagcgggaga atgacgaagc ggatactgac gcttagcctt cgcattggtct gttgtttcgg

```

2003041 cttgcaccgt tccatccaga ttttaggggtg agcaaccgtc agcaacgtgg ccgtcctggc
 2003101 aaagtctttt cctgtcctca ccttcagctc ctttatttcc cactgtggag cctaataccgg exon 2 of
 2003161 caccatcca gaacgcagct cccgctccat cggctgcccc acgtcgtcgg aactttgcag RvY_02619
 2003221 ccagtcatgc cgccaatgtc gacctgccag gctccgtttg gcacggggaa acctggggag
 2003281 atcaacatga tccgccgaac cgattagcag ctgatgtcga caacttcgac **tg**gagatcga **Trp** codons
 2003341 aattc**tg**gct gggcaag**tg**g agctctatcc cagagaagga tcaaaatttg gaggcttacc
 2003401 ttgctgtcat gggtaagccg gagacttacg cttgattgac tgtcattgat tgactggcctt
 2003461 ccaacttcog cttccgggtt caacaggtgt cgac**at**gaac catcccaaca tgaagaagga SAHS12
 2003521 tcaacccgtt acacttcaga ccttcaagaa gggtgacaag taccatcata agatcgtggg "start"
 2003581 cgaggaagcc ggctacatta acgat**g**taag tttgatggac ctggcagctt tcttcagcc
 2003641 ggatgtcatg ttgctttatc cgacgcgaat gtagtaacgc ctttcattt actccatggt
 2003701 gtgccgtaat ggagaagcgt ggcgataaca tgcgtgtgat acgcatggta ttccggacag
 2003761 ggaggcctat gtgtcctttt attgttattc caggttattt tccgcctcgg ccgagagact
 2003821 cccgatctt ataacggtca acagatcact gtcaactatg aggaacaagg cgtgctttg
 2003881 gtgggtaccg tcaagtatcc cgcccataac aaggtcatcc ataataccta cgagatggat
 2003941 gggcagaatc tggccaag**gt** atcaaacctt acttctctt ttgcagcttt tttcctggaa
 2004001 acgcccgtct gacaatttgc tgacagcggg gctcgtttgt tgcagacttc cgaatgtgag
 2004061 ggtgtcgttc acaagcgctg gtataacaag cagcaaaa**act** gaagcctgtc gcctccatta
 2004121 attgtgatag ttttgcttc gagttacgat tcctcatgaa agtgcttttc atgtatgtct
 2004181 gccattttaa ctaactgtac cagatgttga tttacggttt tggatagctg cagtattcct
 2004241 tcagagaact ttgcgatgca acgaaccatg ttccttcttt gtccactgtg aatacgaatg
 2004301 gctgcgatct actatggaag cactgcctac gtagagaaaa ccgaaaatgt cctgcctcag
 2004361 aactagtttc cagtttcccta gacatttcga caccctccag tatctttctc gcttaggggtg
 2004421 tcgcacgaac agaaactaca gttctaactg cgcctttcgg cggctgactt cgcattcga

Supplementary Computational Simulation Methods

Overview. The goal of these simulations was to provide potential insight into the transition of SAHS1 from its primarily beta-sheet structure to some other structure that it might adopt upon desiccation. To this end, we generated an AlphaFold prediction of the structure and interactions of a set of three SAHS1 proteins, and then simulated the behavior at a very high temperature, 550 Kelvin, for 1 microsecond. This simulation indicated that alpha helices can transiently form and disappear, and that most of the amino acids are converted to a coil conformation as defined by their phi/psi backbone angles. The structures do not reach an equilibrium state.

The simulation conditions do not completely replicate the biological process that we are trying to understand, which likely plays out over hours instead of microseconds, and which likely involves rather gradual withdrawal of water, Brownian collisions with unrelated proteins (*in vivo*), and denaturation that may be driven by loss of material within the cavity of SAHS1 instead of by high temperatures. For example, we performed circular dichroism measurements after dialyzing our protein overnight into the denaturing agent trifluoroethanol (TFE). The simulation we performed was designed to be exploratory and might represent part of the denaturation process and illustrate how alpha helices might be nucleated from a disordered structure, but the other aspects of desiccation are not easily simulated with current technology.

AlphaFold structure prediction. We used AlphaFold2 [7]. The starting structure predicted for the trimer is provided as a supplementary file.

Predicted structures were generated for 1, 2, 3, 4, 8, and 16 SAHS1 molecules, and various structural complexes with varying degrees of plausibility were revealed. The choice of

using three SAHS1 proteins for simulation was to strike a balance between capturing protein-protein interactions while not building an inefficient simulation system for long timescales.

In addition, the AlphaFold structure for three copies of SAHS1 predicted that an N-terminal tail of this protein would fit into the cavity of another SAHS1 protein. This is illustrated in Figure S10.

Comparison of the three different SAHS1 proteins in the simulation. To save on computational time, rather than performing separate simulations we performed a single simulation with three copies of the SAHS1 protein present in a water bath. The results, illustrated in Figure S8, were similar for each copy of SAHS1 and indicated that the amino acid psi/phi angles in each protein went from a ~50% to ~0% beta conformations within 20-40 nanoseconds, to almost completely coiled conformations in the same period, and showed a slight increase in alpha helical conformations that peaked at about 40 nanoseconds and was roughly constant thereafter.

Simulation details.

number of simulations	1 simulation with 3 protein copies
simulation box dimensions	100 Å cube
total number of atoms	124,411
total number of water molecules	39,038
salt concentration	74 x Cl ⁻ ions and 83 x Na ⁺ (neutral charge)
Amino acid protonation state	Typical for amino acid side chains at pH 7.5

Solvation box details. A 100 Å simulation box with TIP3 water as solvent was generated using Ambertools and the amber forcefield (ff14SB) (<https://ambermd.org/doc12/AmberTools13.pdf>; <https://ambermd.org/Manuals.php>). Na⁺ and Cl⁻ ions were added to achieve a neutral charge. Simulations were performed using Openmm 7 (<http://docs.openmm.org/7.7.0/developerguide/>), periodic boundary conditions, and a Particle-

Mesh Ewald with a cutoff of 1*nanometers and an Ewald error tolerance of 0.0005. A Monte Carlo barostat was used at 1-atmosphere pressure and an interval of 25 using the Langevin Integrator. Following equilibration at 310 K, the simulation was extended from a restart checkpoint, and velocities reset to the 550 K temperature.

Secondary structure assignments. The Python package MDTraj was used. Specifically, the protein secondary structure (DSSP) secondary structure assignments function (https://mdtraj.org/1.9.4/api/generated/mdtraj.compute_dssp.html). This function implements the assignment based on the reference [8].

The simplified version was executed, which groups the secondary structure into helical, strand, and coil. “Helical” includes Alpha helix, 3-helix (3/10 helix), and 5 helix (pi helix). “Strand” includes residues in isolated beta-bridge and extended strands, participating in beta ladders. The coil includes hydrogen-bonded turns and bends.

Supplementary References

1. Malki, A. *et al.* Intrinsically Disordered Tardigrade Proteins Self-Assemble into Fibrous Gels in Response to Environmental Stress. *Angew. Chem. Int. Ed.* **61**, e202109961 (2022).
2. Yagi-Utsumi *et al.* Desiccation-induced fibrous condensation of CAHS protein from an anhydrobiotic tardigrade. *Sci. Rep.* **11**, 21328 (2021).
3. Yamaguchi, A. *et al.* Two novel heat-soluble protein families abundantly expressed in an anhydrobiotic tardigrade. *PLoS One* **7**, e44209; 10.1371/journal.pone.0044209 (2012).
4. Fukuda, Y., Miura, Y., Mizohata, E. & Inoue, T. Structural insights into a secretory abundant heat-soluble protein from an anhydrobiotic tardigrade, *Ramazzottius varieornatus*. *FEBS Lett.* **591**, 2458-2469 (2017).
5. Fukuda, Y. & Inoue, T. Crystal structure of secretory abundant heat soluble protein 4 from one of the toughest “water bears” micro-animals *Ramazzottius varieornatus*. *Protein Sci.* **27**, 993-999 (2018).
6. Hashimoto T. *et al.* Extremotolerant tardigrade genome and improved radiotolerance of human cultured cells by tardigrade-unique protein. *Nat. Commun.* **7**, 12808; 10.1038/ncomms12808 (2016).
7. Jumper, J. *et al.* Highly accurate protein structure prediction with AlphaFold. *Nature* **596**, 583-589 (2021). <https://github.com/google-deepmind/alphafold>
8. Kabsch, W. & Sander, C. Dictionary of protein secondary structure: pattern recognition of hydrogen-bonded and geometrical features. *Biopolymers: Original Research on Biomolecules* **22**, 2577-2637 (1983).